Accepted for publication in the Astrophysical Journal
Preprint typeset using LaTeX style emulateapj v. 11/26/04

THE ACS VIRGO CLUSTER SURVEY XI. THE NATURE OF DIFFUSE STAR CLUSTERS IN EARLY-TYPE GALAXIES[1]

Eric W. Peng [2], Patrick Côté [2], Andrés Jordán [3,4], John P. Blakeslee [5,6], Laura Ferrarese [2], Simona Mei [5], Michael J. West [7], David Merritt [8], Milos Milosavljević [9,10], and John L. Tonry [11]

Accepted for publication in the Astrophysical Journal

ABSTRACT

We use HST/ACS imaging of 100 early-type galaxies in the ACS Virgo Cluster Survey to investigate the nature of diffuse star clusters (DSCs). Compared to globular clusters (GCs), these star clusters have moderately low luminosities ($M_V > -8$) and a broad distribution of sizes ($3 < r_h < 30$ pc), but they are principally characterized by their low mean surface brightnesses which can be more than three magnitudes fainter than a typical GC ($\mu_g > 20$ mag arcsec^{-2}). The median colors of diffuse star cluster systems are red, $1.1 < g - z < 1.6$, which is redder than metal-rich GCs and often as red as the galaxy itself. Most DSC systems thus have mean ages older than 5 Gyr or else have super-solar metallicities implying that diffuse star clusters are likely to be long-lived, surviving for significant fraction of a Hubble time. We find that 12 galaxies in our sample contain a significant excess of diffuse star cluster candidates. Nine of them are morphologically classified as lenticulars (S0s), and five of them visibly contain dust. We also find a substantial population of DSCs in the halo of the giant elliptical M49, associated with the companion galaxy VCC 1199. Most DSC systems appear to be both aligned with the galaxy light and associated with galactic disks, but at the same time many lenticular galaxies do not host substantial DSC populations, and environment and clustercentric radius do not appear to be good predictors of their existence. Diffuse star clusters in our sample share similar characteristics to those identified in other nearby lenticular, spiral, and dwarf galaxies. Unlike luminous GCs, whose sizes are constant with luminiosity, DSCs are bounded at the bright end by an envelope of nearly constant surface brightness. We suggest that populations of diffuse star clusters preferentially form, survive, and coevolve with galactic disks. Their properties are broadly consistent with those of merged star cluster complexes, and we note that despite being 3–5 magnitudes brighter than DSCs, ultra-compact dwarfs have similar surface brightnesses. The closest Galactic analogs to the DSCs are the old open clusters. We suggest that if a diffuse star cluster population did exist in the disk of the Milky Way, it would be very difficult to find.

Subject headings: galaxies: elliptical and lenticular, cD — galaxies: evolution — galaxies: star clusters, globular clusters: general — open clusters and associations: general

1. INTRODUCTION

In the Milky Way, star clusters have long been divided into two distinct classes—ancient globular clusters (GCs) that populate the halo and bulge, and the young and less massive open clusters that reside in the disk. Globular clusters appear to be a ubiquitous stellar population, present in galaxies of nearly all morphological types, luminosities, and star formation histories. Studies of extragalactic GCs over the past decade, especially with the Hubble Space Telescope (*HST*), have revealed properties that are uniform or slowly varying across galaxies—their distributions of size, color, and luminosity.

Some observations of nearby spiral, irregular, and lenticular galaxies, however, have revealed a wider array of star cluster characteristics, all of which are ultimately windows onto the galactic environment within which they form and reside. In addition to GCs, these galaxies also contain star clusters for which there are no Galactic analogs, for example the young "populous" star clusters in the Magellanic Clouds and M33 that are intermediate in mass between open and globular clusters and do not fit the Galactic dichotomy (e.g. Chandar, Bianchi, & Ford 1999). In M101 and NGC 6946, *HST* imaging reveals a larger than expected number of faint, compact, old star clusters that are similar to GCs but have numbers that continue to rise at luminosities fainter than the typical turnover value of the globular cluster luminosity function (Chandar, Whitmore, & Lee 2004).

HST imaging has also uncovered a different population

[1] Based on observations with the NASA/ESA *Hubble Space Telescope* obtained at the Space Telescope Science Institute, which is operated by the Association of Universities for Research in Astronomy, Inc., under NASA contract NAS 5-26555.

[2] Herzberg Institute of Astrophysics, National Research Council of Canada, 5071 West Saanich Road, Victoria, BC V9E 2E7, Canada; Eric.Peng@nrc-cnrc.gc.ca, Patrick.Cote@nrc-cnrc.gc.ca, Laura.Ferrarese@nrc-cnrc.gc.ca
[3] European Southern Observatory, Karl-Schwarzschild-Str. 2, 85748 Garching bei München, Germany; ajordan@eso.org
[4] Astrophysics, Denys Wilkinson Building, University of Oxford, 1 Keble Road, OX1 3RH, UK
[5] Department of Physics and Astronomy, Johns Hopkins University, Baltimore, MD 21218, USA; jpb@pha.jhu.edu, smei@pha.jhu.edu
[6] Department of Physics and Astronomy, Washington State University, Pullman, WA 99164, USA
[7] Department of Physics and Astronomy, University of Hawaii, Hilo, HI 96720, USA; westm@hawaii.edu
[8] Department of Physics, Rochester Institute of Technology, Rochester, NY 14623-5604, USA; merritt@astro.rit.edu
[9] Theoretical Astrophysics, California Institute of Technology, Mail Stop 130-33, Pasadena, CA 91125, USA; milos@tapir.caltech.edu
[10] Sherman M. Fairchild Fellow
[11] Institute for Astronomy, University of Hawai'i, 2680 Woodlawn Drive, Honolulu, HI 96822, USA; jt@ifa.hawaii.edu

of faint and unusually extended old star clusters in two lenticular galaxies NGC 1023 and NGC 3384 (Larsen & Brodie 2000; Larsen et al. 2001). These clusters (which the authors call "faint fuzzies") appear to be moderately metal-rich ([Fe/H] ~ -0.6), have old ages (> 7 Gyr) and are both spatially and kinematically associated with the stellar disks of the lenticular galaxies in which they were serendipitously discovered (Brodie & Larsen 2002). However, they find that neither the S0 galaxy NGC 3115 nor the elliptical NGC 3379 seems to possess a similar population.

Extended clusters that appear atypical for the Milky Way have also been identified in M31 (Huxor et al. 2005) and M33 (Chandar et al. 1999), and appear particularly numerous in M51 (Chandar et al. 2004). Sharina, Puzia, & Makarov (2005) also find a large fraction star clusters that are fainter and more extended than typical GCs in nearby dwarf galaxies (D = 2–6 Mpc), both dSphs and dIs. van den Bergh (2005a) combine the Sharina et al. (2005) data with that for low-luminosity galaxies in the Local Group find that dwarf galaxies have an excess of faint old star clusters as compared to giant galaxies. Most recently, Gómez et al. (2005) have found that GCs in the peculiar elliptical galaxy NGC 5128 (Cen A) have sizes and ellipticities that extend to higher values than their Milky Way counterparts.

What are the conditions that give rise to these star clusters? The constituents of cluster systems are a direct reflection of the variegated formation histories of the parent galaxies—the numbers and masses of star clusters is proportional to the star formation rate density (Larsen & Richtler 2000), while the survival of these clusters is dependent on their compactness, their orbits, their age, and the local gravitational potential (e.g. Fall & Rees 1977; Zhang & Fall 2001). By investigating the nature of star cluster systems for which there are no or few known Local Group analogs, we are studying a much wider array of star forming environments and galactic evolutionary histories.

At present, it is unclear whether the star clusters in these galaxies are all the result of the same phenomena, or are formed and destroyed through many different processes. Some appear metal-poor (M31; Huxor et al. 2005) and some metal-rich (NGC 1023, 3384). Many appear associated with galactic disks, but at least a few in M33 are not. Fellhauer & Kroupa (2002) have proposed that these star clusters can be formed through the merging of star cluster complexes, and may be related to the hierarchical nature of star formation in disks (Bastian et al. 2005). Some of these clusters also may not be all that different from Milky Way GCs or open clusters. Observationally, however, they share one common property—the accumulating evidence for this newfound diversity in extragalactic star cluster systems is a direct result of our ability to study fainter and lower surface brightness star clusters in other galaxies. Being able to resolve the sizes of these clusters is essential to all these studies.

In this investigation, we present a study of low surface brightness or "diffuse" star cluster (DSC) populations in the ACS Virgo Cluster Survey (ACSVCS, Côté et al. 2004, Paper I). The ACSVCS is a program to image 100 early-type galaxies in the Virgo cluster with the HST Advanced Camera for Surveys (ACS). This survey is designed to study the star cluster systems of these galaxies in a deep and homogeneous manner. Moreover, the high spatial resolution afforded by HST/ACS enables us to measure sizes for all star clusters (Jordán et al. 2005). As such, the survey is well-designed to determine the properties of star clusters that have lower surface brightnesses than typical globular clusters, and to determine their frequency in early-type galaxies.

2. OBSERVATIONS AND DATA

2.1. *The Sample*

A full description of the ACS Virgo Cluster Survey is provided in Paper I. Here, we briefly describe the sample and observations. The ACSVCS is a program which obtained HST/ACS images in the F475W (g) and F850LP (z) filters of 100 early-type galaxies from the Virgo Cluster Catalog (VCC) of Binggeli, Sandage, & Tammann (1985, hereafter BST85). These galaxies were selected to be certain or probable members of the Virgo cluster excluding the Southern Extension, have $B_T < 16$, and morphologically classified as E, S0, dE, dE,N, dS0, or dS0,N. From these 163 galaxies, we were required to trim to a sample of 100 because of time limitations, eliminating 63 galaxies that were S0 or dwarfs with uncertain or disturbed morphologies, significant dust, lacking a visible bulge, or had prior HST/WFPC2 imaging. We note that despite this culling, this early-type sample is magnitude limited for the brightest 26 galaxies with $B_T < 12.15$ ($M_B < -18.94$), and that 38 of the 100 galaxies in our sample are classified as S0, E/S0, or S0/E (see Paper I for the full list of galaxies and their properties). For the purposes of this paper, we adopt a distance to the Virgo Cluster of $D = 16.5$ Mpc with a distance modulus of 31.09 ± 0.03 mag from Tonry et al. (2001), corrected by the final results of the Key Project distances (Freedman et al. 2001; see also discussion in Mei et al. 2005).

All observations were taken with the Wide Field Channel (WFC) of the ACS. The WFC has two 2048×4096 CCDs butted together with a scale of $0\farcs049$ pixel^{-1} and a field of view of $202'' \times 202''$. At the distance of the Virgo Cluster, this translates into 4 pc pixel^{-1} and a 16.2 kpc $\times$ 16.2 kpc field of view. Exposure times in the F475W and F850LP filters totaled 720 sec and 1210 sec, respectively.

2.2. *Data Reduction*

Our ACS/WFC images were reduced using a dedicated pipeline which is described in Jordán et al. (2004a,b, Papers II and III). The science images are produced by combining them and cleaning them of cosmic rays using the Pyraf task *multidrizzle* (Koekemoer et al. 2002). In order to detect star clusters, it is first important to remove the light from the galaxy. We subtract a model of the galaxy in each filter and subsequently iterate with the source detection program SExtractor (Bertin & Arnouts 1996) in order to mask objects and remove any residual background. We do our final object detection using estimates of both the image noise and the noise due to surface brightness fluctuations. Objects are accepted into our catalog only if they are detected in both filters. Very bright or elongated objects are rejected to eliminate obvious foreground stars and background galaxies. For the remaining objects we use the program KINGPHOT

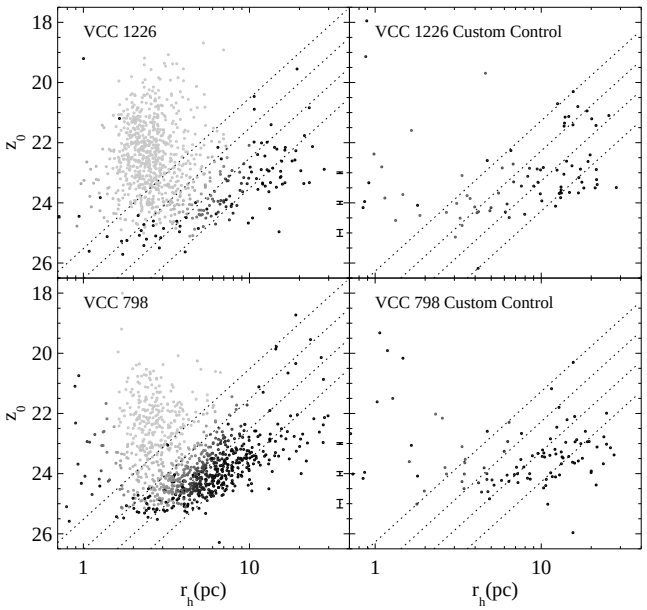

FIG. 1.— Size-magnitude selection diagrams and control fields for VCC 1226 (M49, top) and VCC 798 (M85, bottom). Gray points with a mean half-light radius of $r_h = 2.6$ pc are objects that likely belong to the traditional population of globular clusters. Black points represent objects classifies as likely to be contaminants. The left panels show the data for the the galaxy fields, and the right panels show what is expected from the custom control field for each galaxy. Diagonal dotted lines are lines of constant mean surface brightness, $\mu_z = 18$, 19, 20, 21 mag arcsec^{-2} (left to right). Notice that VCC 798, despite having a smaller GC population than VCC 1226, has many more objects in the "contaminant" locus than would be expected from the control fields. These lower surface brightness objects are the star clusters of interest. Error bars represent the median photometric error at those magnitudes. Median errors in r_h for those bins are 0.26, 0.57, and 1.22 pc, respectively.

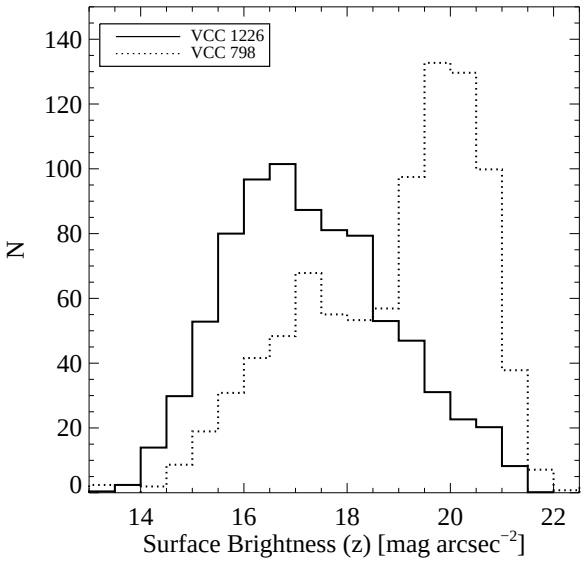

FIG. 2.— Histograms of z surface brightness for objects in VCC 1226 (solid) and VCC 798 (dotted). Expected background galaxy contamination as measured in the custom control fields has been subtracted. As in Figure 1, compared to VCC 1226, VCC 798 has a large population of star clusters with lower surface brightnesses ($z \gtrsim 19$ mag arcsec^{-2}).

(Jordán et al. 2005) to measure magnitudes and King model parameters for all candidate star clusters. KINGPHOT fits King model surface brightness profiles convolved with the point spread function (PSF) appropriate for each object in each filter. For total magnitudes, we integrate the flux of the best-fit PSF-convolved model to the limit of the PSF and apply an aperture correction that is dependent on the fitted half-light radius, r_h (see description in Peng et al. 2005, Paper IX). Magnitudes and colors are corrected for foreground extinction using the reddening maps of Schlegel, Finkbeiner, & Davis (1998) and extinction ratios for the spectral energy distribution of a G2 star (Paper II; Sirianni et al. 2005). For the purposes of this paper, we use g and z to mean the ACS magnitudes g_{475} and z_{850}.

2.3. *Control Fields*

A critical issue in any extragalactic star cluster study that pushes to faint apparent magnitudes is contamination from background galaxies. In Peng et al. (2005), we described an approach where we run our pipeline on 17 blank, high-latitude control fields taken from the ACS Pure Parallel Program (GO-9488 and 9575). Even with equivalent exposure time, however, it is important to remember that blank fields will always detect fainter objects than our ACSVCS images because the bright galaxy in our science images necessarily creates a spatially varying detection efficiency that is a function of the background light. We address this issue by creating "custom" control samples for each galaxy. To do this, we run the detection on each control field as if that particular Virgo galaxies were in the foreground. In this way, we are able to create a true comparison sample tailored to each ACSVCS galaxy.

2.4. *Star Cluster Selection*

In Paper IX, we used our carefully constructed control samples to optimally identify globular clusters. Our ability to measure sizes for objects provides leverage in the size-magnitude plane to separate globular clusters from other objects. The control fields allow us to localize the contaminating population in this plane (mostly background galaxies). Typical GCs have median half-light radii of $r_h \sim 3$ pc (e.g. Jordán et al. 2005) and follow a Gaussian-like luminosity function. On the other hand, the contaminant population consists of point sources at all magnitudes (foreground stars), and a background galaxy population that consists of faint, compact galaxies as well as brighter, more extended galaxies. This is demonstrated in the top panel of Figure 1 which shows the r_h–z_0 diagram for the brightest galaxy in our sample, M49 (VCC 1226), as well as its custom control field. We assign each object in this diagram a "GC probability" based on its position relative to the loci of GCs (assumed) and contaminants (measured). Objects with GC probabilities greater than 0.5 are included in our GC sample. We describe the details of the algorithm in Paper IX and Jordán et al. (2006).

It is important to note, however, that the GC and contaminant loci have the highest degree of overlap for objects that have low surface brightnesses ($\mu_z \gtrsim 19$ mag arcsec^{-2}), where μ_z is the mean surface brightness within the half-light radius. Therefore, faint or extended star clusters are not easily separated from background galaxies on the basis of magnitude and size alone. While in Paper IX, we purposely focused our study on

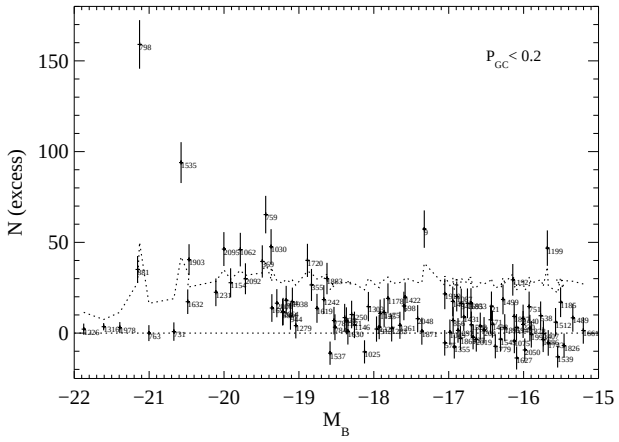

FIG. 3.— Number of "non-GCs" versus galaxy absolute B magnitude. We show the number of objects with GC probabilities less than 0.2 and $r_h > 4$ pc that are in excess of what is expected for the background as estimated from the control fields. Numbers alongside the points are the VCC numbers for each galaxy. The dotted line represents a three-sigma value in the excess distribution. Note that while VCC 798 is the largest outlier, a number of galaxies, notably around $M_B = -20$, have a significant excess of objects in this region of parameter space.

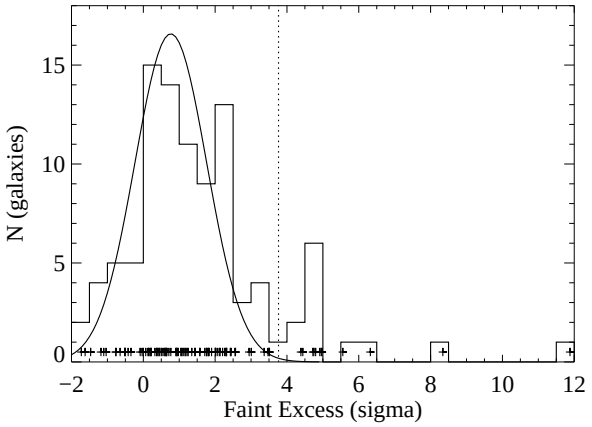

FIG. 4.— Distribution of "non-GC" excess in units of sigma over the background. Data is the same as for Figure 3. The expected width of the distribution as determined by counting statistics and cosmic variance is represented by the Gaussian curve. While the mean has been adjusted to fit the galaxy data, its width has not. Pluses along the bottom represent the position of individual galaxies. Notice that the distribution is largely Gaussian, but has a tail of objects to the right. The dotted line represents 3σ above the mean, and separates "normal" galaxies from those that have an excess of faint, extended objects.

the "traditional" GC population, the focus of this paper is to investigate the existence and properties of star clusters that have lower surface brightnesses than typical GCs, and that are more easily confused with background objects. Therefore, for the purposes of this paper, we define this sample as all objects with GC probabilities less than 0.2 and half-light radii $r_h > 4$ pc. We set this strict criteria so that we may avoid contamination from the sample of traditional GCs. While the exact numbers for this cutoff are not critical, we chose these values because they are inclusive of many objects yet the background corrected numbers for this cut is still close to zero for most galaxies (i.e. they are uncontaminated by GCs even for the massive ellitpicals).

3. RESULTS

3.1. *The Existence and Frequency of Diffuse Star Cluster Populations*

We can test each galaxy for the existence of a population of diffuse star clusters (DSCs) by comparing the total number of objects in this region of the size-magnitude plane with that expected from the control fields. When we do this, we find that some galaxies have a clear excess of objects in this locus. Figure 1 shows a comparison between the normal giant elliptical VCC 1226 (M49) and the S0 galaxy VCC 798 (M85). Diagonal dotted lines are loci of constant z surface brightness, μ_z. While the number of objects with low GC probabilities (< 0.2) in VCC 1226 is consistent with that in the custom control sample, the number of these objects in VCC 798 — those with $\mu_z \gtrsim 19$ mag arcsec^{-2} — is well in excess of the background.

This is further illustrated in Figure 2 where we show the background subtracted μ_z distributions for all star cluster candidates in VCC 1226 and 798. VCC 798 has a large population of star clusters at lower surface brightnesses, and of the 100 galaxies in the ACSVCS sample, VCC 798 has the largest number of DSC candidates. Note that the turnover of the surface brightness distribution at $\mu_z \sim 20$ is due to incompleteness and not an intrinsic property of the objects themselves.

In Figure 3, we show the number of "non-GCs" that are in excess of the expected background for the entire ACSVCS sample. Most of the galaxies have almost no excess population of objects. This shows that our custom control fields are in fact providing reasonable estimates of the background. It is also the case that galaxies with both large and small numbers of globular clusters can have excesses near zero, showing that our chosen criterion of $P_{GC} < 0.2$ is stringent enough to eliminate most of the traditional GC sample from appearing our sample of potential DSCs.

In the figure, we also plot a dotted line that represents the point at which the number of objects are in excess of the background at a level greater than 3σ above the mean. The expected variance for each galaxy is determined using the 17 control fields. We count the number of objects that meet the selection criteria in each field and determine the variance of this number over all the control fields. This is then added to the variance expected from Poisson counting statistics in the science field itself. Figure 4 shows a histogram of galaxies, binned by the diffuse source excess in units of σ. While the mean of the distribution is slightly shifted (around 0.8σ), the width of the distribution is fixed by our error bars, and thus the fact that a unit Gaussian is a reasonable match to the distribution shows that our error bars are also reasonable.

Figure 4 also shows that there is a significant tail of galaxies that have very high numbers of low surface brightness sources. In addition to VCC 798 and VCC 1535 which Figure 3 shows to have the largest number of sources in excess of the background, there are a total of twelve galaxies that have an excess greater than 3σ. These galaxies and some of their properties are listed in Table 1. For the purpose of investigating the nature of the diffuse star cluster populations, we focus this paper

TABLE 1
GALAXIES WITH $> 3\sigma$ EXCESS OF $P_{GC} < 0.2$ SOURCES

VCC (1)	M_B (2)	$(g–z)_{galx}$ (3)	Type(VCC) (4)	$(g–z)_{DSC}$ (5)	N_{DSC} (6)	$S_{N,DSC}$ (7)	$T_{L,DSC}(z)$ (8)
881	−21.2	1.51	S0/E	1.27	32	0.09	1.2
798	−21.1	1.32	S0	1.33	160	0.36	4.2
1535	−20.6	···	S0	1.54	93	0.40	4.7
1903	−20.5	1.46	E	1.40	38	0.17	2.1
2095	−20.0	1.39	S0	1.29	48	0.34	3.6
1062	−19.8	1.48	S0	1.48	45	0.30	3.7
369	−19.5	1.47	S0	1.48	37	0.38	5.0
759	−19.4	1.46	S0	1.49	65	0.55	7.0
1030	−19.4	···	S0	1.37	47	0.52	6.1
1720	−18.9	1.40	S0	1.43	38	0.51	7.2
9	−17.3	1.06	dE	1.11	59	4.20	46.4
1199	−15.7	1.52	E	1.42	45	24.44	352.6

[1]Number in Virgo Cluster Catalog
[2]Absolute B Magnitude, extinction-corrected, $D = 16.5$ Mpc
[3]Galaxy color from Paper VI
[4]Morphological type from the VCC
[5]Median color of DSCs
[6]Number of DSCs
[7]Specific frequency of DSCs: $S_{N,DSC} = N_{DSC} \times 10^{0.4(M_V+15)}$
[8]Specific z luminosity of DSCs: $T_{L,DSC}(z) = L_{z,DSC}/L_{z,galaxy} \times 10^4$

on these twelve galaxies that have $> 3\sigma$ excesses of faint, extended sources. However, we note that a number of galaxies that have less significant excesses also possibly harbor populations of DSCs.

We show the size-magnitude (r_h–z_0) diagram for each one of these twelve galaxies and their custom control fields in Figure 5. The objects that are likely to be GCs are gray, while objects that would normally be classified as contaminants are black. In each case, there is an excess of low surface brightness objects over what one sees in the custom control field. The galaxies are ordered by their total B luminosity, and we point out that fainter galaxies have fainter objects included in their custom control fields, as one would expect with the lower average background. It is also clear that for most galaxies at the distance of the Virgo Cluster, there is a substantial background population and one must be very careful drawing conclusions about the existence of DSCs without a careful treatment of the background. This is a problem in *apparent* magnitude, so will be less of an issue for more nearby star cluster systems, and more of problem for more distant star cluster systems.

Of the twelve galaxies that have a significant population of DSCs, nine of them are classified as S0 or S0/E: VCC 881, 798, 1535, 2095, 1062, 369, 759, 1030, and 1720. Of the three galaxies that were not classified as S0 by BST85: VCC 1903 is classified as an E5 in the RC3 (de Vaucouleurs et al. 1991); VCC 9 is a low surface brightness galaxy that appears atypical for its luminosity—it is a dwarf with a "core" and is possibly a dI/dE transition object; and VCC 1199 is a companion of VCC 1226 (M49), only 4.′5 away, and it is likely that most of the star clusters we see belong to the cluster system of the nearby giant elliptical. Five of the galaxies (all of them S0s) also visibly contain dust—VCC 881, 798, 1535, 759, and 1030.

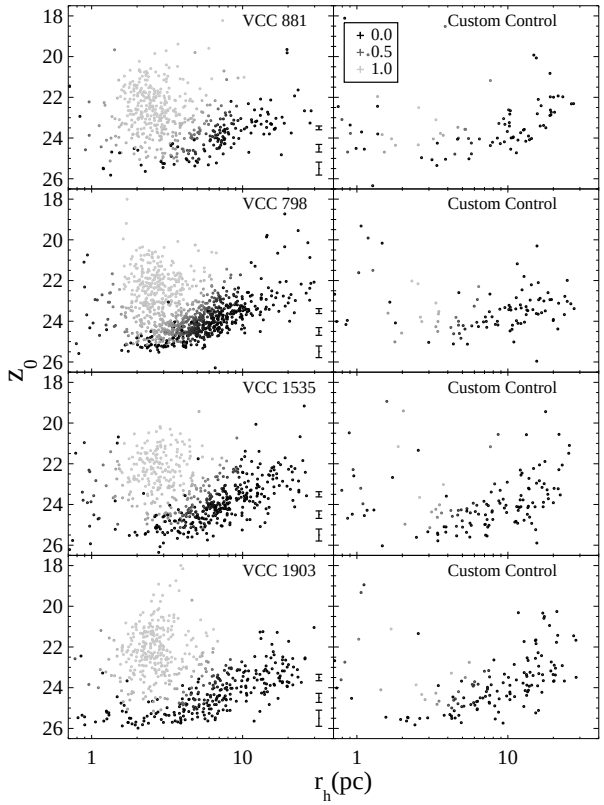

FIG. 5.— Size-magnitude diagrams for the twelve galaxies that have significant diffuse source excesses, listed in Table 1. Using the algorithm described in the text, we assign a GC probability based on its position in the r_h–z_0 diagram. Objects are color coded by their probability of being a globular cluster. On the left are the objects in our program fields, and on the right are the objects in the custom control fields for that galaxy, scaled to a single field. Each one of these galaxies shows at least a 3σ excess of diffuse sources as compared to the control fields.

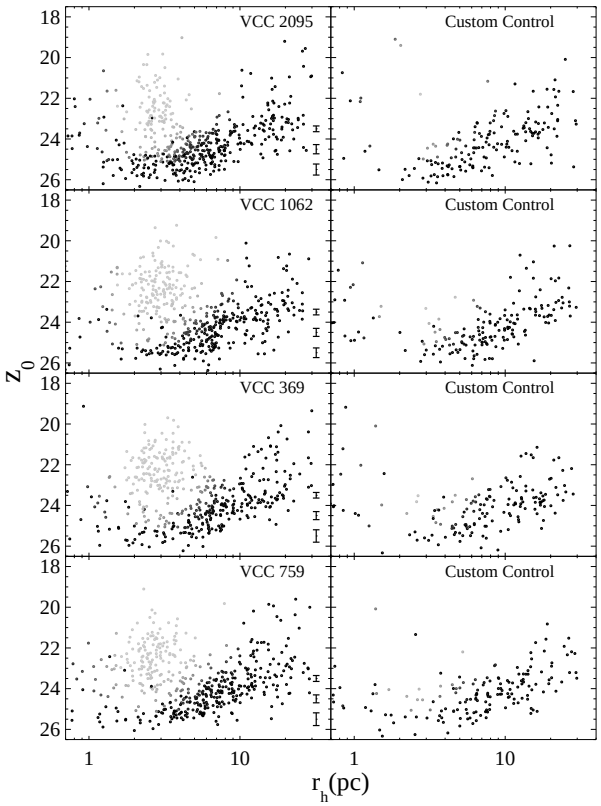

FIG. 5.— continued. Size-magnitude diagrams for the twelve galaxies that have significant diffuse source excesses.

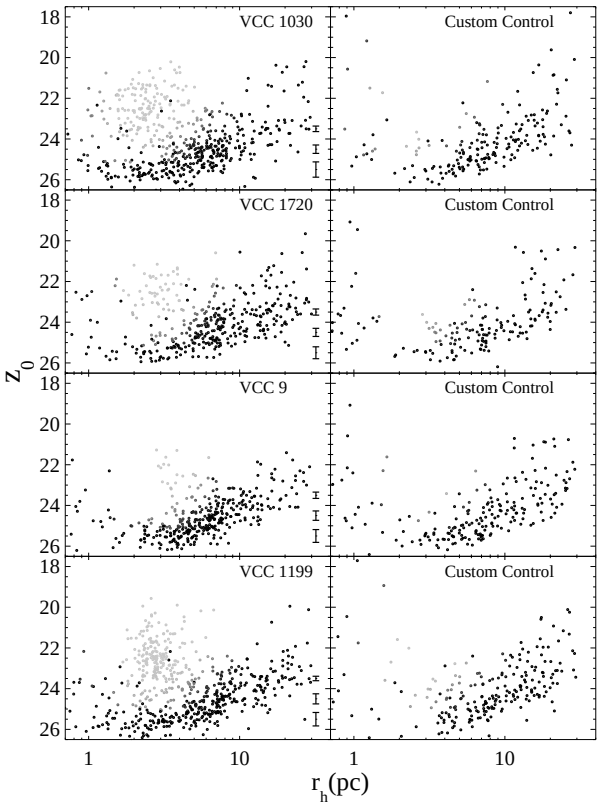

FIG. 5.— continued. Size-magnitude diagrams for the twelve galaxies that have significant diffuse source excesses.

3.2. *Properties of Diffuse Star Clusters: Colors, Magnitudes, Sizes*

Although the diffuse star clusters have sizes and magnitudes similar to the background galaxy population, their color distributions may be very different. For all twelve "excess" galaxies, we show in Figure 6 the color distributions of all DSC candidates with the color distributions of the expected contaminant population from the custom control fields (scaled to the area of one field). We find that the DSCs are generally *redder* than the background. In most cases, the color distributions of objects with $(g–z) < 1.0$ are well-matched by the colors of objects in the control sample. However, at redder colors, there is a clear excess of objects. This argues that the DSC candidates cannot simply be a result of an underestimated background that has a higher cosmic variance than expected.

A background cluster of galaxies, it may be argued, could also give rise to an excess of red objects. However, in Figure 7, we show the spatial distribution of red and blue DSC candidates (divided at $(g–z) = 1.0$) around the highly inclined S0 galaxy, VCC 2095. The red objects appear highly clustered around the disk of the galaxy, despite the lower detection efficiency in those regions (due to the galaxy light). The blue objects are distributed more randomly about the field. This argues that the red and diffuse objects are in fact star clusters associated with the galaxy. We discuss the spatial distribution of the DSCs around the other galaxies in Section 3.3.

How do the colors of the DSCs compare to the other star clusters in these galaxies, the globular clusters?

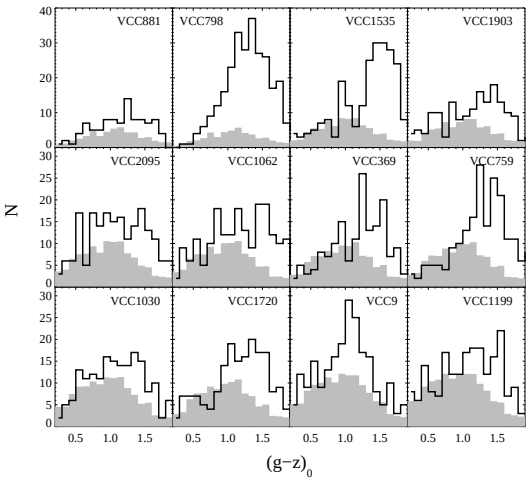

FIG. 6.— Color distributions of diffuse sources (black) compared to that for expected background contamination (filled gray) for the 12 galaxies in Table 1. Galaxies are ordered by decreasing B luminosity. All histograms use 0.1 mag bins. Notice that the colors of the diffuse sources are redder than that the typical background contaminant. While the distribution of diffuse sources bluewards of $(g–z)_0 \sim 1.0$ is generally well-matched by the control fields, these galaxies clearly harbor an excess of red sources.

Once we take into account the expected contamination from background galaxies, we can derive a statistically corrected color distribution. Figure 8 shows the corrected DSC color distributions for all twelve galaxies, and the median color for each. Also shown are the GC color distributions for the same galaxies. In most galaxies, it is possible to see the bimodality in the GC color distribu-

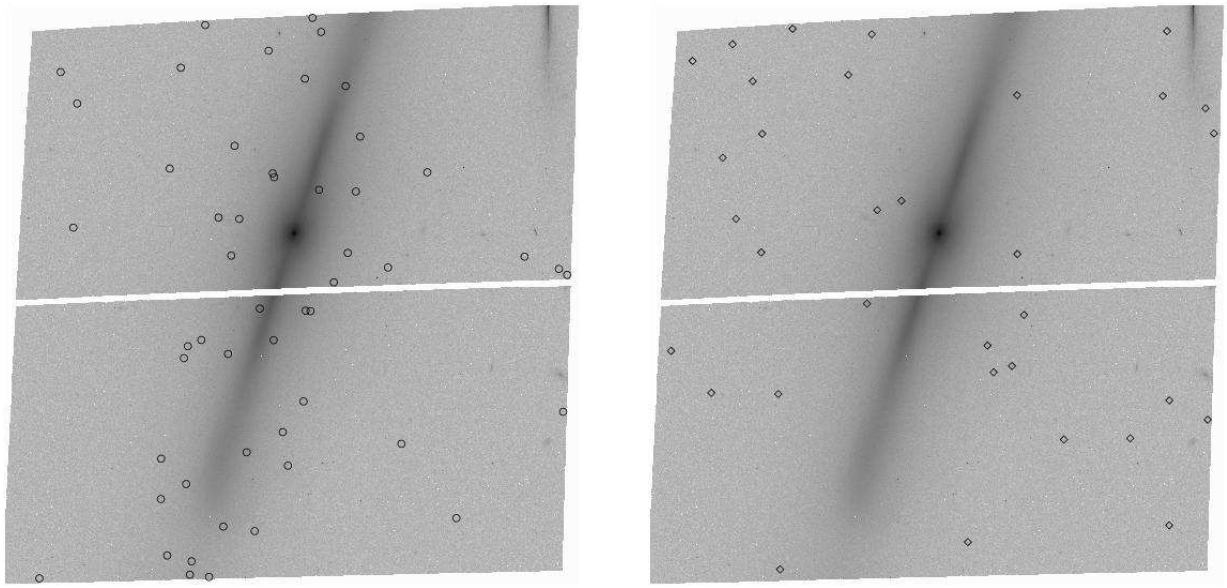

FIG. 7.— Spatial distributions of diffuse sources around VCC 2095, one of the most edge-on galaxies in our sample. Sources are divided by color at $(g–z)_0 = 1.0$. Red sources (*left*) are generally in excess of the background, while blue sources (*right*) are consistent with background levels seen in control fields. The red sources are spatially clustered around the disk of the galaxy, supporting the idea that they are intrinsic to the galaxy. Blue sources are scattered more randomly through the field.

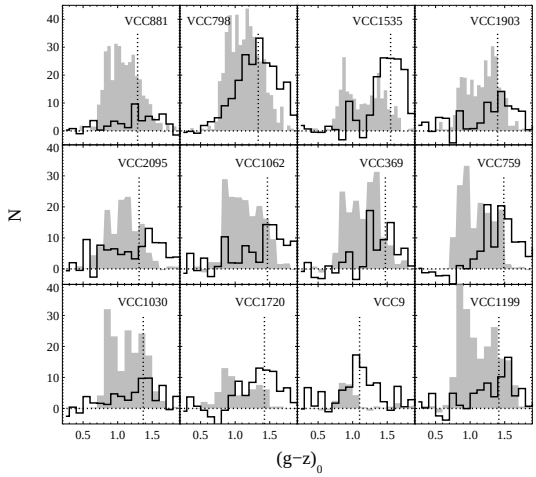

FIG. 8.— Color distributions of diffuse star clusters (black) compared to colors of globular clusters (filled gray) for the 12 galaxies in Table 1. Galaxies are ordered by decreasing B luminosity as in Figure 6. All distributions have been subtracted for the expected contamination from foreground and background sources. All histograms use 0.1 mag bins except for the GCs for the four brightest galaxies (top row), which are binned in 0.05 mag intervals. Vertical dashed lines mark the median color of the diffuse sources. This population is typically redder than even the red GC subpopulation.

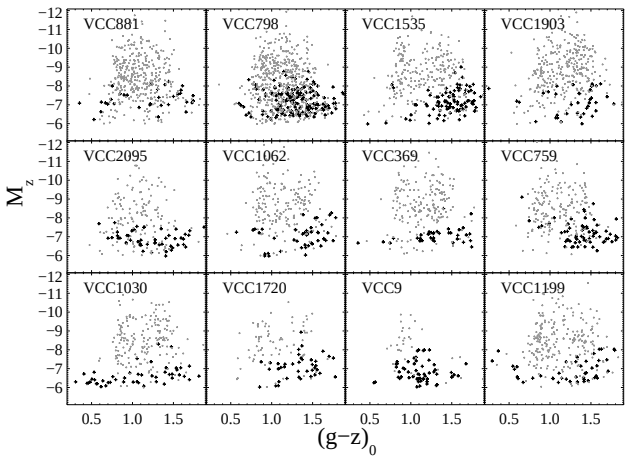

FIG. 9.— Color–magnitude diagram, $(g–z)$–M_z, of globular clusters (gray or red) and diffuse star clusters (black) in the twelve galaxies listed in Table 1. Both samples have been statistically cleaned of background objects using control fields. Globular clusters have $P_{GC} > 0.5$, while the diffuse cluster population is defined to have $r_h > 4$ pc and $P_{GC} < 0.2$. The diffuse population is typically fainter than the turnover of the GC luminosity function, and as red or redder than the red GCs.

tion (Paper IX). In all cases, the median color of the DSCs is as red or redder than the red GC subpopulation. These median color values are listed in Table 1. All of these values are redder than the background objects in our control fields, which have median colors of $(g–z) = 1.0$.

These properties are also displayed in Figures 9 and 10 where we show the color-magnitude and color-surface brightness relationships for the star clusters in all twelve galaxies. In both figures, we compare the DSC and GC populations. All plots have been statistically cleaned for background contamination using a "nearest neighbor" approach — for each object in a randomly selected subset of the control catalog (one in seventeen for the 17 control fields), we remove the object in our source catalogs that is closest in the parameter space. In Figure 9, we see that the DSCs are fainter and redder than the GCs. Figure 10 shows color against μ_z, and the diffuse star clusters again generally appear redder, although this is not universally true for all galaxies. All twelve galaxies have red DSCs, but some also have a number of blue objects (in the case of VCC 1903, some are very blue). At these colors, contamination and Poisson noise from the background is more severe, so it is difficult to draw conclusions about the nature of these objects.

3.3. *Spatial Distributions of DSCs*

By selecting only red DSC candidates $(g–z > 1.0)$, we can decrease the contaminant fraction and investigate

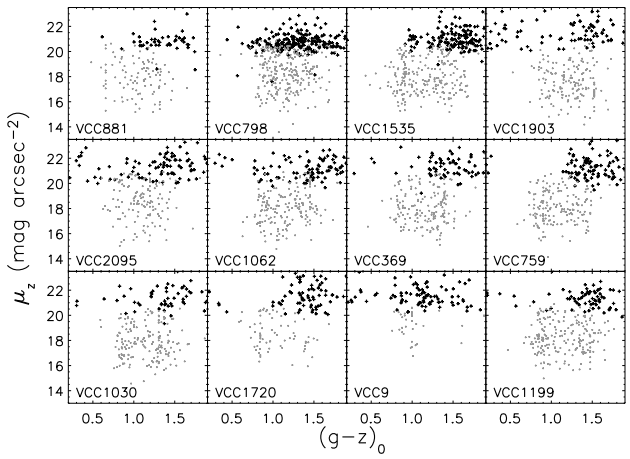

FIG. 10.— Color–surface brightness diagram, $(g–z)_0$ versus μ_z, of globular clusters (red) and diffuse star clusters (black) in the twelve galaxies listed in Table 1. Data are the same as for Figures 5 and 9. The diffuse clusters often have very red colors, although some galaxies have diffuse clusters with a wide range of colors.

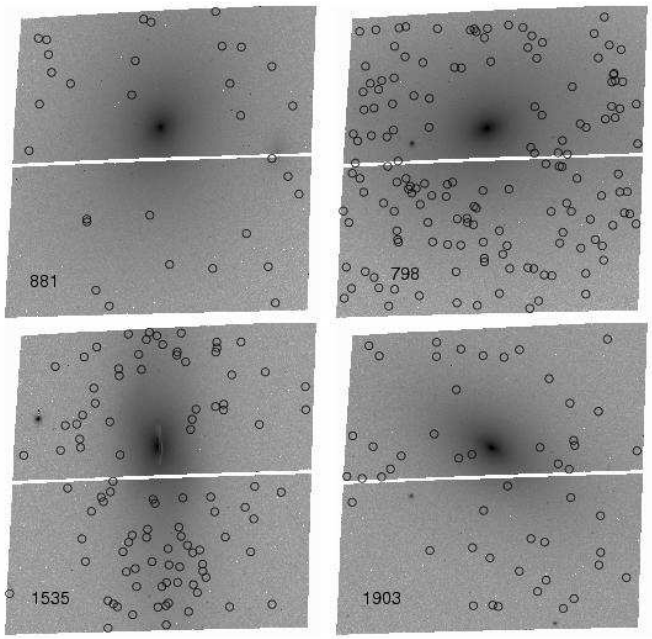

FIG. 11.— Spatial distribution of red ($g–z > 1.0$), diffuse cluster candidates around galaxies with significant excesses. While some of the objects are in the background, the large majority are likely star clusters. For obviously inclined or elliptical galaxies, it is possible to see that the spatial distribution of the clusters appears to follow the underlying galaxy light. The VCC numbers of the galaxies are shown in the lower left.

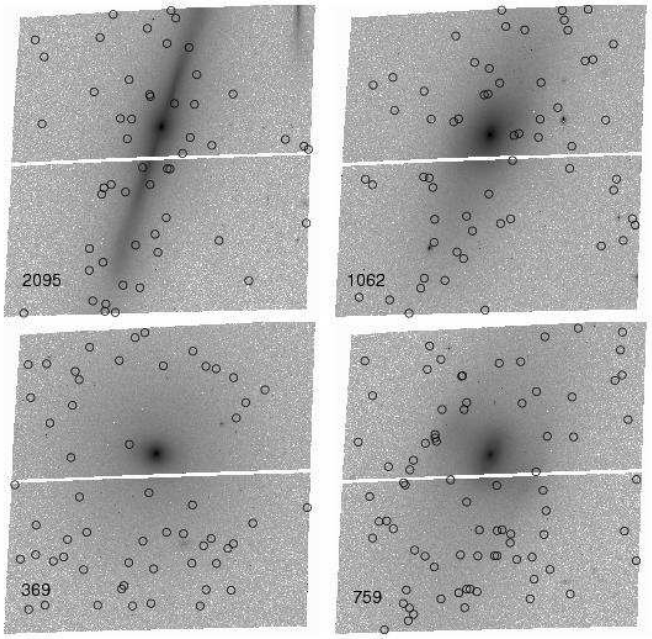

FIG. 11.— continued. Spatial distribution of red ($g–z > 1.0$), diffuse cluster candidates around galaxies with significant excesses.

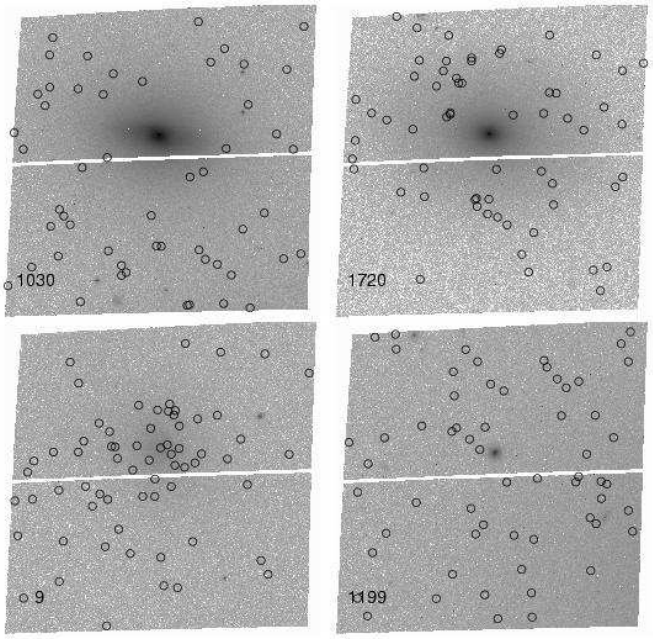

FIG. 11.— continued. Spatial distribution of red ($g–z > 1.0$), diffuse cluster candidates around galaxies with significant excesses.

the spatial distribution of the DSCs. Figure 11 shows the positions of the red DSCs plotted on the ACS/WFC images of the twelve "excess" galaxies. In galaxies that are significantly inclined or where the light distribution is anisotropic, we find that the DSCs also have an anisotropic distribution. This particularly appears to be the case for VCC 1535, 2095, 1062, and 1720. Alignment with the galaxy light in S0s suggests that the DSCs are associated with the stellar disks of the galaxies, rather than the halos. We note that when we restrict ourselves to only red DSC candidates, two more galaxies meet our criteria of having a 3σ excess over the mean—VCC 1154 and VCC 2092, both of which are classified as S0s, and one of which (1154) harbors a large kiloparsec-scale central dust disk.

Previous work on "faint fuzzy" clusters in NGC 1023 and 3384 (Larsen & Brodie 2000; Brodie & Larsen 2002) suggested that they were not only associated with the stellar disks of these galaxies, but that they resided in a *ring* around the galaxy, avoiding the central regions. This has many astrophysical implications if true (Burkert, Brodie, & Larsen 2005) so we wished to test this for the diffuse star clusters in the ACSVCS data.

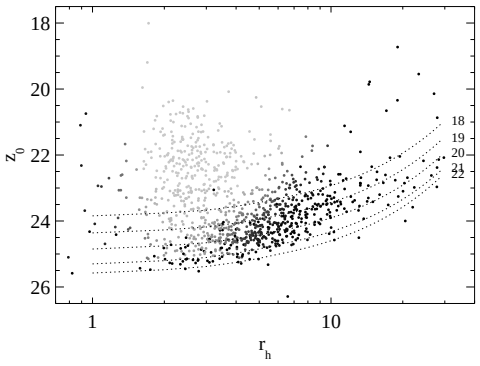

FIG. 12.— Size-magnitude diagram for VCC 798 with 90% completeness curves for different galaxy surface brightnesses. This plot is the same as the bottom left of Figure 1 except that we have now overplotted our 90% completeness curves for underlying galaxy surface brightnesses of $\mu_{z,galaxy}$ = 18, 19, 20, 21, and 22 mag arcsec^{-2} as labeled. Notice that at $\mu_{z,galaxy} = 19$, most of the diffuse clusters become difficult to detect. In Figure 13, we show where this isophotal surface brightness level lies in the galaxy.

Because the central regions of galaxies have the highest surface brightnesses, it is natural that we should detect fewer objects there. We estimate the detection efficiency in our images by adding artificial star clusters at a range of magnitudes, half-light radii, and background surface brightnesses. We then run our detection algorithm on the images and record the fraction that are recovered. We are thus able to characterize the detection probability in this three-dimensional parameter space.

In Figure 12, we show the size-magnitude diagram for VCC 798, the galaxy with the largest number of DSCs. We overplot the 90% completeness curves in this plane for a range of background surface brightnesses. In the bright central regions of the galaxy with $\mu_{z,galaxy} <$ 19 mag arcsec^{-2}, although over half of the GCs are still detected, almost all of the DSC candidates fall below the detection threshold. Figure 13 shows the ACS/WFC F850LP image of VCC 798 with the locations of the DSC candidates. The central ellipse corresponds to the location of the $\mu_{z,galaxy} = 19$ mag arcsec^{-2} isophote using data from Ferrarese et al. (2005). The deficit of DSCs within this isophote is due to incompleteness. Thus, our data are not deep enough to determine whether DSCs exist in the central regions of VCC 798 and other luminous galaxies. We do have one lower surface brightness galaxy with a large number of DSCs, VCC 9, and Figure 11 shows that we detect numerous DSCs clustered around that galaxy's center. VCC 9, however, appears different from the other galaxies in a number of ways, however, so its properties may not be extendable to the rest of the sample.

3.4. *Specific Frequencies and Luminosities of DSCs*

The number of star clusters usually scales with the total luminosity of the galaxy. For globular clusters, it is sometimes useful to talk in terms of specific frequency, a quantity scaled to unity for 1 GC in a galaxy of $M_V = -15$. Likewise, we would like to compare not just total numbers of diffuse star clusters, but the number per unit galaxy luminosity in order to investigate the efficiency of DSC formation. In Table 1, we list an "observed" specific frequency, $S_{N,DSC}$, which is simply

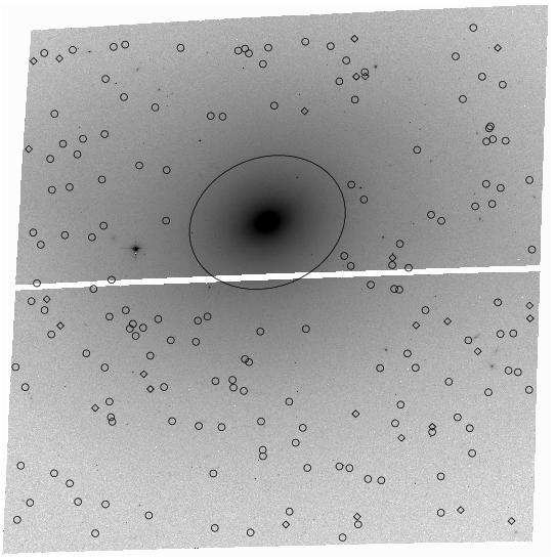

FIG. 13.— F850LP (z) image of VCC 798 with diffuse objects and a $\mu_{z,galaxy} = 19$ mag arcsec^{-2} isophote overplotted. Inside this ellipse, we do not find any diffuse clusters, but this is likely because our detection efficiency is rapidly becoming low, and not necessarily because of any intrinsic deficit of clusters toward the galaxy center.

$N_{DSC} \times 10^{0.4(M_V+15)}$, where N_{DSC} is the number of diffuse star cluster candidates that we observe in excess of the background. The galaxy magnitudes that we use are the total measured g and z band fluxes observed *within the ACS/WFC aperture*. Because we do not observe the entire galaxy, the best we can do is compute specific frequency within the ACS/WFC field of view.

For GCs, the luminosity function is well-approximated by a Gaussian, so it is meaningful to talk about total numbers of GCs. In the case of the DSCs, we do not know the form of their luminosity function, so the number that we observe is highly dependent on the depth of the observation. For both GCs and young massive clusters in spiral galaxies, though, most of the luminosity is in the brightest objects (i.e. the bright ends of their luminosity functions follow a power-law with exponents > -2). This is why the specific luminosity of a star cluster system is often a more robust quantity. Following Larsen & Richtler (2000) and Harris (1991), we calculate the DSC specific luminosity in the z-band, which is proportional to ratio of the luminosity in diffuse clusters to the galaxy's luminosity — $T_{L,DSC}(z) = L_{z,DSC}/L_{z,galaxy} \times 10^4$. We find that the fraction of galaxy light in DSCs for the nine lenticular galaxies to be 1–7×10^{-4}. When normalized to galaxy luminosity, the galaxy with the highest number of DSCs, VCC 798, does not appear particularly special with $T_{L,DSC} = 4.2$. The real outliers are VCC 9 and 1199. This is to be expected for VCC 1199 if the star clusters we see are really part of the M49 system. VCC 9's very high specific luminosity of DSCs suggests that it was either more efficient at producing DSCs, or that it was once a more luminous system.

If specific luminosities of diffuse star cluster systems is relatively constant across galaxies, then our 3σ criterion will make us insensitive to DSC systems in faint galaxies where the noise is dominated by background galaxies. For instance, if the faintest galaxy in our sample (VCC 1661) had the same specific frequency as VCC 1720

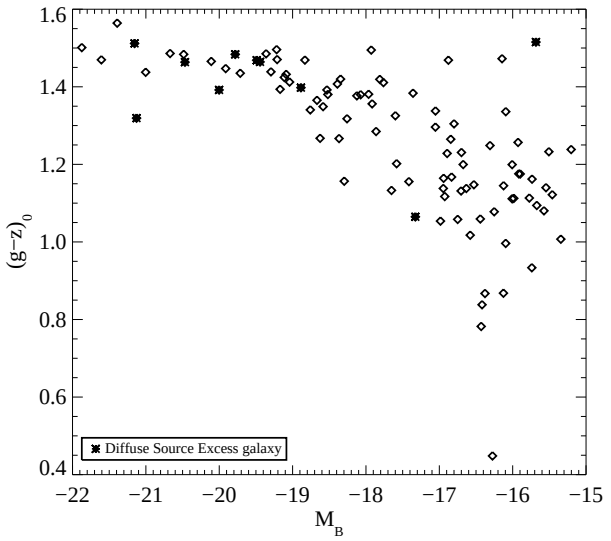

FIG. 14.— Color-magnitude diagram of galaxies with an excess of diffuse sources, compared to the rest of the ACSVCS sample. Colors are from Paper VI and absolute B magnitudes are from BST85 assuming a distance of 16.5 Mpc. While two of the galaxies appear to be significantly bluer than the mean color-magnitude relation (VCC 798 and VCC 9), other galaxies with DSCs do not have colors that distinguish themselves from normal galaxies. VCC 1199 in the upper left is a companion of M49 (VCC 1226) and is known to be much redder than expected for its luminosity.

(0.51), then we would only expect it to have 0.6 diffuse clusters. Thus, the dwarfs in our sample may have a few DSCs, but it is nearly impossible to draw firm conclusions.

3.5. *Properties of Galaxies with Diffuse Star Clusters*

3.5.1. *Morphology*

To try to understand the origin of the DSC population, we looked at the different properties of the host galaxies. Most of the galaxies that have significant numbers of diffuse star clusters are lenticular (S0) galaxies, pointing to a possible connection to the existence of a stellar disk. The spatial clustering around the disks of inclined galaxies supports this view. However, there are many S0 galaxies in our sample that do *not* show significant diffuse star cluster populations. Figure 3 shows a grouping of galaxies with $-19.5 < M_B < -19$, many of which have S0 morphological classifications, but none of which have a very significant number of DSCs. This corroborates the findings of Larsen et al. (2001) who also found that while the two lenticulars NGC 1023 and 3384 had "faint fuzzies", another lenticular, NGC 3115, did not possess them, implying that they are not a universal phenomenon in S0 galaxies.

To make a comparison between similar galaxies that have different DSC properties, we create a comparison sample of eight intermediate luminosity early-type galaxies with $-19.5 < M_B < -19$ of which seven are classified as S0, E/S0 or S0/E (Table 2), and all of which have low numbers of DSC candidates. The median excess above the mean level for faint, extended sources in these galaxies is 0.9σ. This is compared to a sample of galaxies with DSCs that are in the magnitude range $-20.1 < M_B < -18.8$ which have a median excess of 4.2σ above the mean value. We limit the magnitude range of the two samples to make a meaningful comparison between the globular cluster populations because we know that the properties of the galaxies and their GC systems vary with galaxy luminosity (e.g. Gebhardt & Kissler-Patig 1999; Paper IX). Interestingly, only one of these galaxies, VCC 685, contains any visible dust.

TABLE 2
COMPARISON GALAXIES

VCC (1)	M_B (2)	$(g_{475}-z_{850})_0$ (3)	Type(VCC) (4)
1692	−19.4	1.51	S0/E
2000	−19.3	···	E/S0
685	−19.2	1.46	S0
1664	−19.2	1.39	E
654	−19.2	1.48	S0
944	−19.1	1.47	S0
1938	−19.1	1.46	S0
1279	−19.0	···	E

[1]Number in Virgo Cluster Catalog
[2]Absolute B Magnitude, extinction-corrected, $D = 16.5$ Mpc
[3]Color from Paper VI
[4]Morphological type from the VCC
[5]Morphological type from the NED

While morphology is a clue, it is not the full story. In Figure 14 we plot the color-magnitude diagram for all ACSVCS galaxies and compare them to the galaxies with significant numbers of DSCs. If the existence of DSCs is related to recent episodes of star formation, we might expect that these galaxies would have bluer than average colors. This appears to be the case for VCC 798 and VCC 9, but the other galaxies do not show any significant deviation from the color-magnitude relation of early-type galaxies. VCC 1199 is a companion of VCC 1226 (M49) and is much redder than expected for its luminosity.

3.5.2. *Globular Clusters*

Likewise, we might expect that the color distributions of globular clusters in galaxies with and without an DSC population might be substantially different. Figure 15 shows the combined GC color distributions for the DSC and comparison galaxy samples. Both distributions are bimodal with the mean colors of the blue peaks very similar. The mean color of the red GCs appears slightly redder in the DSC galaxy sample. The most notable difference is that the fraction of red GCs is lower in the comparison sample, a value of 0.45 as opposed to 0.56 for the galaxies with DSCs. This, however, may be a result of the larger luminosity range for the galaxies with DSCs, particularly the inclusion of VCC 1903 which has a very high fraction of red GCs (0.61) and contributes $\sim 30\%$ (269/911) of the GCs to that group.

3.5.3. *Environment*

Another factor that may play some role in the existence of DSCs is the local environment. Galaxies such as VCC 798 and 1030 have nearby companion spiral galaxies. VCC 798 is almost certainly interacting with the neighboring SBb galaxy, NGC 4394, which lies at a distance of $7\farcm6$ (37 kpc, projected). VCC 798 also exhibits fine structure that are indications of a recent interaction (Schweizer & Seitzer 1992). VCC 1030 is $4\farcm4$ (21 kpc,

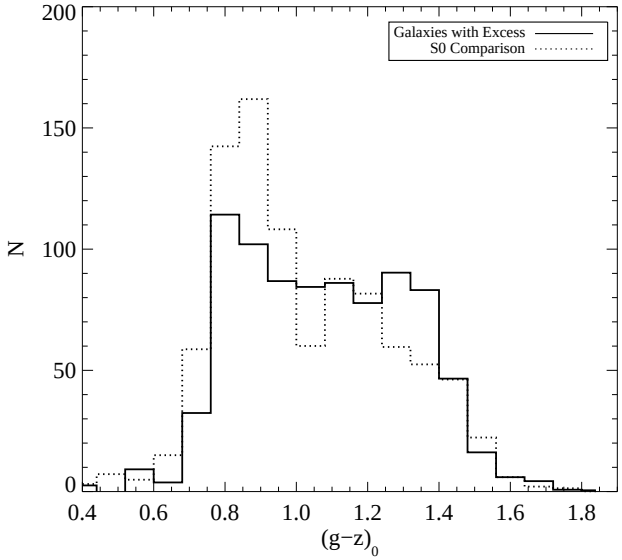

FIG. 15.— Combined globular cluster color distributions for S0 galaxies with and without a significant population of diffuse clusters. We choose only galaxies with $-21.1 < M_B < -18.8$ to create a more uniform comparison. The comparison sample of S0s is listed in Table 2. Both distributions appear bimodal and the means of the two peaks are very similar. The galaxies with DSCs may have a slightly redder red peak, and an excess of red GCs, but this may also be due to the larger luminosity range of these galaxies, in particular the inclusion of VCC 1903 which has a significant red GC subpopulation.

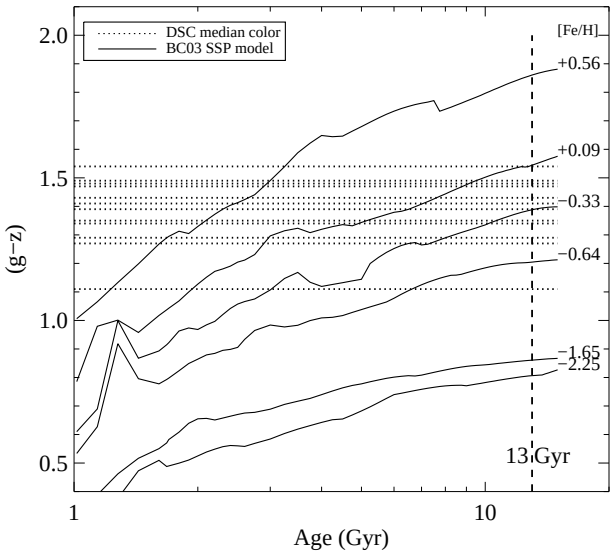

FIG. 16.— Comparison of the colors of diffuse clusters with simple stellar population (SSP) models of Bruzual and Charlot (2003). Solid lines represent isometallicity SSP tracks showing the evolution of $(g–z)$ with age from 1–15 Gyr. The vertical dashed line marks an age of 13 Gyr. Horizontal dotted lines mark the median colors of the DSC populations from Table 1. With the exception of VCC 9, which has the bluest color, most DSC populations must either have old ages (> 5 Gyr) or metallicities substantially in excess of solar.

projected) from NGC 4438 (VCC 1043), an S0/a galaxy with a very disturbed morphology. Other galaxies such as VCC 9, whose nearest neighbor in the VCC has a projected distance of 81 kpc, are very isolated.

The first diagnostic of density in a galaxy cluster is the projected distance to the cluster center. For the Virgo Cluster, we take the position of the cD galaxy M87 (VCC 1316) to be the center of the cluster at $(\alpha, \delta)_{J2000} = (12{:}30{:}49.43,\ +12{:}23{:}28.35)$. We do not detect any significant trend with clustercentric radius, except perhaps for the fact that the galaxies with the two largest excesses (VCC 798 and 1535) are far from the center of the cluster.

We also use the Virgo Cluster Catalog (BST85) to define a metric of the local environmental density. We use all galaxies in the VCC that are certain or probable members of the cluster, and by determining the distance to the first, fifth, and tenth nearest neighbor we can calculate the local surface density of galaxies within that radius. We do not find correlations between any of these density indicators and the number of DSCs. So, despite the clues given to us by VCC 798 and 1030, it does not appear that local galaxy density is a strong indicator of the existence of DSCs.

4. DISCUSSION

4.1. *The Ages and Metallicities of DSCs*

Like most star clusters, DSCs are likely to be simple stellar populations (SSPs), so even though we only have a single color with which to constrain their properties, we can compare them to models and still gain reasonable constraints on their possible ages and metallicities. In Figure 16, we plot isometallicity tracks for SSPs from the models of Bruzual & Charlot (2003) using a Chabrier (2003) initial mass function. We use SSP models because there are no good empirical measurements of star clusters in $(g–z)$ that cover a sufficient range in age and metallicity. For five different metallicities, the models show how the $(g–z)$ color of SSPs become redder as the population ages from 1 to 15 Gyr. Overplotted are lines representing the median colors of the DSC populations from Table 1. With the exception of VCC 9 which has by far the bluest DSC population, *all the DSC systems must either have old (> 5 Gyr) ages or metallicities in excess of solar.* Even for super-solar metallicities, it is very unlikely that the DSCs have mean ages younger than 2 Gyr. Using a Salpeter IMF makes the models redder by about 0.04 mag but does not change the general conclusion. For VCC 1535, the reddest DSC system, even with an age of 13 Gyr the clusters must have [Fe/H] = +0.09. We note that VCC 1535 does harbors a central dust disk, and although the DSCs are well beyond the visible dust in our images we cannot rule out the possibility that there might be some reddening that is unaccounted for. However, there is no systematic color difference for DSCs in galaxies with and without visible dust. Nevertheless, we caution that with only two filters we are vulnerable to any internal extinction that may exist.

We also find that the colors of the DSCs appear to closely track the colors of their parent galaxy. For half of the sample, the median DSC color is almost exactly the color of the galaxy, implying that the two stellar populations coevolved. While the age-metallicity degeneracy prevents us from drawing definitive conclusions, if we make the assumption that the ages of the clusters are between 8 and 13 Gyr, then their metallicities span a range of approximately $-0.3 <$ [Fe/H] $< +0.1$. The only exception is VCC 9, whose DSCs must have [Fe/H] $\gtrsim -0.8$, but could also have ages of ~ 2 Gyr at solar metallicity.

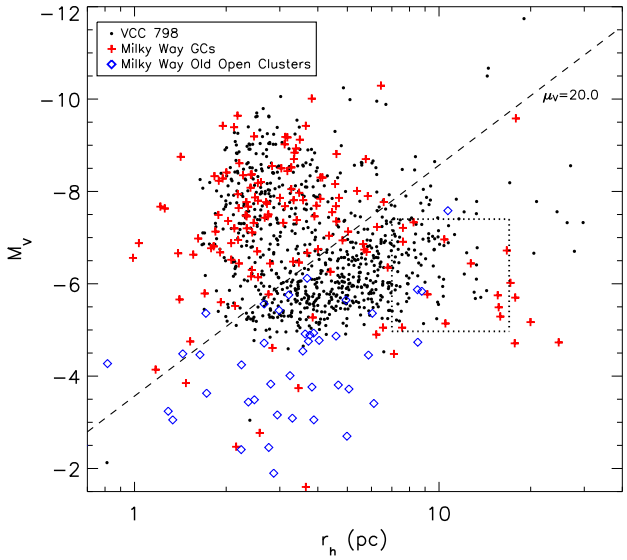

FIG. 17.— Size-magnitude diagram for star clusters in VCC 798 (dot), Milky Way globular clusters (cross), Milky Way old open clusters (diamond), and "faint fuzzy" selection box from Larsen & Brodie (dotted lines). The VCC 798 catalog was statistically cleaned of background contamination, and photometry was transformed to M_V using the relations in the text and a distance of 16.5 Mpc. The dashed line represents a constant mean surface brightness, $\mu_V = 20$ mag arcsec^{-2}, below which most DSCs lie. The locus of GCs in VCC 798 match the GCs in the Milky Way with the exception of the low surface brightness Galactic halo GCs which would fall below our detection threshold (lower right). Most of the Milky Way old open clusters would also fall below our detection threshold. The brightest of these clusters, however, would have the sizes and magnitudes of DSCs in our sample. In the Galaxy, there is a deficit of objects in the DSC locus. The "faint fuzzy" region selects the more extended DSCs.

4.2. *Comparisons with the Milky Way*

One frequently raised question in the study of these diffuse star clusters is whether they are truly different from the star clusters found in the Milky Way. Some of the fainter globular clusters are quite extended, with half-light radii of $7 < r_h < 30$ pc, and outer halo GCs are known to span a large range in surface brightness (e.g. van den Bergh & Mackey 2004). These GCs, though, are associated with the halo and are much more metal-poor than the DSCs appear to be. Open clusters are found in the Galactic disk and are fainter than globular clusters so provide a tempting parallel. Most open clusters are unlike DSCs, though, in that they are only a few hundred Myr old. The old open clusters, with ages of 0.7–12 Gyr (Janes & Phelps 1994), might be more similar. The combination of the diffuse star clusters being old, metal-rich, *and* low surface brightness makes them different from most known Milky Way analogs. In Figure 17, we show the size-magnitude diagram for all star cluster candidates (GC and DSC) in VCC 798, the system in our sample with the largest number of DSCs. In order to facilitate comparisons with other published data, we transform our ACS g and z magnitudes to Johnson V. We derive this transformation using the V and I photometry of M87 globular clusters presented in Kundu et al. (1999) and our g and z photometry from the ACSVCS. We do a robust linear fit to the data and obtain

$$V = g + 0.026(\pm0.015) - 0.307(\pm0.013) \times (g - z) \quad (1)$$

$$I = z - 0.458(\pm0.017) + 0.172(\pm0.014) \times (g - z). \quad (2)$$

Figure 17 also shows the locations in this diagram of the Milky Way globular clusters with data taken from the compilation of Harris (1996). Most of the Galactic GCs have r_h around 3 pc and share this region of the diagram with a large number of VCC 798 GCs. The rest of the Galactic GCs, most of which have $V > -6.5$ and $r_h > 5$ pc, have very low surface brightnesses and a large number are below our detection threshold. The locus of the VCC 798 DSCs, a band from (3 pc,−5 mag) to (30 pc,−8 mag), is comparatively devoid of Galactic globular clusters.

We also show the locations of Milky Way old open clusters in this diagram. We use diameters, distances, and reddenings from van den Bergh (2005b), which is based on the catalogs of Dias et al. (2002). We used V photometry from the SIMBAD astronomical reference database. Of the 74 old open clusters listed in Friel (1995), we were able to obtain these data for 44 objects. Ages for these clusters range from 0.8-8 Gyr. Size estimates should be viewed with caution as they are not true half-light radii, but are usually taken to be the radius at which the cluster stellar density matches that of the field. This radius, though, is probably most associated with a half-light radius as opposed to a core or tidal radius (Friel 1995). We caution that the data for this sample are very heterogeneous, but they are sufficient to show that the bulk of the old open clusters are much fainter than the DSCs we are seeing in the ACSVCS. It is also likely that the old open clusters are younger than the DSCs and will fade even more in this diagram. However, the surface brightness distribution of the old open clusters does overlap with that of the DSCs, and it is plausible that the DSCs are in fact just the most luminous objects of a much more massive system of disk clusters that is akin to the old open clusters of the Milky Way. Both deeper observations of external galaxies and a more homogeneous and precise catalog of Galactic open cluster properties will be needed to explore any further connection between DSCs and open clusters.

4.3. *Comparisons with Star Clusters in Other Galaxies*

Because the DSCs appear to be associated with stellar *disks*, perhaps the most interesting comparison is with the old star cluster populations of nearby spiral galaxies. Chandar et al. (2004) conducted a painstaking study of the old star cluster systems of five nearby low-inclination spiral galaxies. Using HST/WFPC2 multicolor imaging, they were able to select a relatively clean sample of old star clusters in the galaxies M81, M83, NGC 6946, M101, and M51, measuring magnitudes, colors, and sizes for 145 GC candidates. In Figure 18 we show the comparison between VCC 798 and the combined sample from these spiral galaxies in the size-magnitude diagram (see Figure 8 in Chandar et al. (2004) for a similar figure labeling star clusters from individual galaxies). Most of these spiral galaxies appear to possess star clusters that populate at least a part of the DSC locus, with M81 and M51 having the largest numbers. It is possible that some of these objects are background contaminants, but this is unlikely

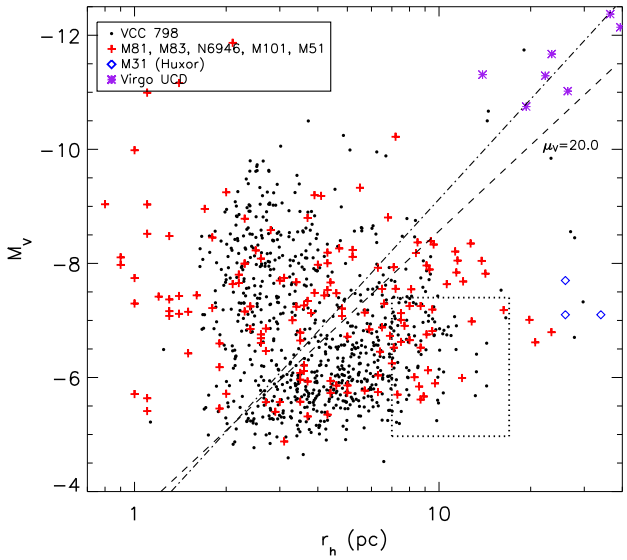

FIG. 18.— Size-magnitude diagram for VCC 798 (dot) with old star cluster candidates (cross) in five spiral galaxies—M81, M83, NGC 6946, M101, M51 (Tables 3–7, Chandar et al. 2004). Photometry for VCC 798 and "faint fuzzy" selection box (dotted lines) is the same as for Figure 17. We also show M31 extended star clusters from Huxor et al. (diamond) and UCDs from Haşegan et al. (asterisk). The dashed line represents a constant mean surface brightness, $\mu_V = 20$ mag arcsec^{-2}. The dash-dotted line represents the mass-radius relation of $M \propto R^{2.33}$ for star cluster complexes in M51 (Bastian et al. 2005). The spiral galaxies possess old star clusters that are similar in size and luminosity to the DSCs in our sample.

— all of these spirals are at least 1.5 mag closer than the Virgo cluster, and the distribution of background galaxies is constant in apparent magnitude. Unlike the DSCs in our sample, however, these star clusters are not predominantly red in color but span the full range of star cluster colors. This is perhaps expected if the color of DSCs is correlated with the color of the underlying stellar disk as these are spiral galaxies still in the act of star formation. Uncertainties in reddening are also likely to be contributing to scatter in the colors.

The "faint fuzzy" star clusters discovered in NGC 1023 and 3384 are in many ways similar to the DSCs. In Figures 17 and 18 we also show the rough selection region that Larsen & Brodie (2000) used to select "faint fuzzy" clusters. In VCC 798, this selection box contains a subset of the DSCs, selecting those that have larger half-light radii. Given the red colors and old ages of the "faint fuzzies" (Brodie & Larsen 2002), it is likely that these populations are the same phenomenon. However, we point out that not all of the DSCs are faint (some have luminosities near the GCLF mean), and some of them are as compact as GCs. The defining characteristic of this "excess" star cluster population is that they are at lower surface brightnesses than the bulk of the globular clusters, hence we refer to this general population as "diffuse" to be as precise and inclusive as possible.

Recently, Huxor et al. (2005) discovered three stars clusters in M31 that are both fairly luminous ($M_V \sim -7$) and extended ($r_h > 25$ pc). When placed in the size-magnitude diagram (Figure 17) we find that while they would be some of the most extended star clusters in VCC 798, they are not so different in size and magnitude from the most extended and luminous DSCs. However, the integrated colors and CMDs of the M31 clusters show that they are blue and metal-poor, making them distinctly different from most of the DSCs, and having perhaps more in common with the Galactic halo GCs. Their large galactocentric radii also suggest that they belong to a halo population.

A recent investigation of the star cluster systems of nearby low surface brightness dwarf galaxies by Sharina et al. (2005) also turned up a number of low surface brightness star clusters that would meet our criteria for DSCs. In their investigation, a majority of the globular cluster candidates in both dwarf spheroidal and dwarf irregular (dI) galaxies can be considered DSCs. The fraction appears higher for the dI galaxies in their sample. This is an interesting complement to our findings because while we do not find many DSCs in the ACSVCS dwarf elliptical galaxies (only VCC 9 has a significant population) this could simply be due to low numbers in each galaxy and a relatively high background. The Sharina et al. sample is much closer (2–6 Mpc) and so suffers much less from the problem of background galaxies. The ACSVCS does not contain dIs, but the presence of diffuse star clusters in dIs might be consistent with them residing in galactic disks.

4.4. *Diffuse Star Clusters in the Milky Way: Lost or Found?*

One of the notable claims made for diffuse star clusters is that there are no known analogs in the Milky Way. However, observations of other nearby disk galaxies with HST as shown in the previous section indicate that such star clusters are not uncommon. This raises the question: if a population of old, metal-rich, diffuse star clusters did exist in the disk of the Milky Way, would we be able to detect them? If so, how many might we expect to find? We can make a zero-order estimate of the number of DSCs we might be expected to have found in the Galaxy. At the distance of the Virgo cluster, the ACS/WFC field of view covers ~ 261 kpc^2 roughly encompassing a galactocentric radius of ~ 8 kpc. If we view a galaxy nearly face on, then we can uses this number to infer a DSC number surface density. The closest analog to DSCs in the Milky Way are the old open clusters in the disk of the Galaxy and we can use their discovery efficiency to determine the likelihood of finding DSCs. Survey efficiency for old open clusters is difficult to quantify, but the observed spatial distribution roughly shows the area in the disk that has been most effectively surveyed. The distribution of old open clusters is most complete between $l = 160°$ and $l = 200°$, and galactocentric radii of 7 to 13 kpc (see Friel 1995). This gives an effective survey area in the disk of 42 kpc^2. The DSCs are more luminous than the old open clusters but are of similar surface brightness, so we expect that their detectability might be roughly similar. If we assume that the mean surface density of diffuse star clusters in our images is an upper limit to that in an annulus from 7–13 kpc, then the number DSCs we might expect to see is a ratio of the areas times the total number in the ACS/WFC field, or $0.16 \times N_{DSC}$. This is the number of DSCs — objects that are detected in our ACSVCS images and classified as a diffuse star cluster — that we would expect to

see in the Milky Way given the extent of old open cluster surveys. If the Galaxy had a DSC population like that in VCC 798, then we might expect to have detected $\lesssim 25$ Milky Way DSCs in open cluster surveys. If the Galaxy has a smaller number of diffuse clusters, like in VCC 1903, then we might only expect to have found $\lesssim 6$ star clusters.

We can also ask the question in reverse — how many old open clusters are known in the disk of the Galaxy that, if placed at the distance of the Virgo cluster and observed in the ACSVCS, would have been classified as a diffuse star cluster? Figure 17 shows that at least nine old open clusters in the Milky Way would have been detected in the ACSVCS if they were in VCC 798. While we realize that old open clusters are not a perfect match for the DSCs and that we have made many simplifying assumptions, these numbers raise two interesting possibilities: 1) The fact that very few analogs to diffuse star clusters have been found in the Galaxy does not necessarily mean that they do not exist. Extrapolating from our survey, we expect that even if the Milky Way had a moderate number of DSCs, only a few might be detectable in surveys done to date, or 2) The number of bright old open clusters may in fact be consistent with the some of the less DSC-rich galaxies that we see.

Ongoing searches for new star clusters with the Two Micron All Sky Survey are currently some of the most promising avenues to discover highly obscured low surface brightness star clusters (e.g. Bica, Dutra, & Barbuy 2003), but these searches are difficult due to variable foreground extinction and high stellar densities in the Galactic disk. A more complete census of disk star clusters, especially for those with large radii, would be invaluable for comparisons to diffuse cluster populations in other galaxies.

4.5. *Constraints on the Origin of the Diffuse Star Clusters*

Fellhauer & Kroupa (2002) have proposed that diffuse star clusters such as the "faint fuzzies" can be formed via the merging of star cluster complexes, which are found in interacting galaxies. Using simulations, they show that star clusters that have the approximate magnitudes and sizes of diffuse star clusters can be formed and survive in a galactic disk for many Gyr. The ultimate evolution of one of these merged star cluster complexes ends up having a surface brightness and luminosity similar to the diffuse clusters we see. They also claim that the same basic process can also form the ultracompact dwarf galaxies (UCDs) that have been discovered in the Fornax and Virgo clusters (Hilker et al. 1999; Drinkwater et al. 2003; Haşegan et al. 2005). In Figure 18, we plot the locations of the Virgo UCDs and dwarf-globular transition objects from Haşegan et al. (2005, 2006).

Observationally, Bastian et al. (2005) observe that young star cluster complexes in the disk of M51 are grouped hierarchically into complexes which show evidence of merging. Unlike star clusters, the complexes show a mass-radius relation which goes as $M \propto R^{2.33\pm0.19}$, which is close to a constant surface brightness (or mass density). Although our data is not complete enough to determine a meaningful surface brightness distribution of DSCs, the fact that the high surface brightness envelope of diffuse star clusters appears to follow a line of nearly constant surface brightness (or $M \propto R^2$) may be a clue to their formation. Bastian et al. (2005) find that the mass-radius relation for giant molecular clouds in M51 is also $M \propto R^2$. In Figure 18, we show both a line of constant surface brightness, $\mu_V = 20$ mag arcsec^{-2}, and a line following the mass-radius relation of Bastian et al. for star cluster complexes which has been fixed to coincide with the Virgo UCDs. While it may be a coincidence, we note that this relation appears to characterize both the UCDs and the upper envelope of the diffuse star clusters.

Although our selection criteria for DSCs in the previous sections does essentially involve a surface brightness cut, the constant surface brightness upper envelope is not a product of our classification. The deficit of objects at this surface brightness shown for VCC 798 in Figures 2 and 18 is independent our our classification scheme. For the fainter and more compact star clusters, it is difficult to separate DSCs from GCs, but it is especially for more extended and luminous star clusters that we see the separation in surface brightness. In galaxies such as VCC 1535, the separation between the DSCs and GCs is clearer. We admit, however, that defining any sort of mass-radius boundary with this data is likely to be uncertain.

We also note that there may more more tha one mechanism for the production of diffuse star clusters. VCC 1199 is a compact elliptical galaxy that lies close in projection to M49, and whose cluster system is likely swamped by that of its giant neighbor. Using a simple model of the M49 GC system one expects that 100–200 GCs in the VCC 1199 field—$\sim$ 50–100% of total—are associated with M49. VCC 1192, another satellite of M49, also has a high number of DSC candidates. Although M49 itself does not appear to have many DSCs, its outer halo appears to have many more. These clusters are not just the more extended GCs one expects to find in the halo as they have the same properties as DSCs in other galaxies. Either they were accreted from other galaxies (such as 1199 and 1192 or others), or perhaps the halo of M49 is more hospitable to the formation and survival of diffuse star clusters.

5. CONCLUSIONS

The ability to obtain deep images of a large sample of nearby galaxies has advanced the study of extragalactic star cluster systems to lower surface brightness levels. Some galaxies have a significant number of diffuse star clusters which appear to be a population apart from globular clusters. Below, we summarize their properties and some constraints on their origins.

1. *Structural Properties.* Diffuse star clusters are characterized by their low surface brightnesses, typically $\mu_g > 20$ and $\mu_z > 19$ mag arcsec^{-2}. Unlike GCs, whose sizes do not vary with their luminosity, the high surface brightness envelope of DSCs is roughly consistent with a constant surface brightness. This hints that DSCs may be bounded by a mass-radius relationship of the type $M \propto R^\gamma$ where $\gamma \approx 2$. The highest surface brightness DSCs are only slightly more diffuse than UCD-like objects.

2. *Diffuse star clusters are old or metal-rich, or both.* The diffuse star clusters tend to have red colors with $1.1 < g - z < 1.6$. Their median colors are redder than the red globular cluster subpopulation, and they often match the color of the galaxy itself. When compared to SSP models, these colors require that all of the DSC systems except those in VCC 9 have mean ages of older than 5–13 Gyr or else have super-solar metallicities. If we assume that they do not have super-solar abundances, then these diffuse clusters are long-lived, and any model for their survival must preserve them for as long as a Hubble time.

3. *Frequency of DSC systems.* We find twelve galaxies in our sample that contain a greater than 3σ excess of diffuse sources above what is expected from the background (Table 1). If we restrict ourselves only to red diffuse sources with $(g–z) > 1.0$, then two more galaxies, VCC 1154 and VCC 2092 also pass this criterion. All of these galaxies with the exceptions of VCC 1903, 9 and 1199 are morphologically classified as lenticulars. The ACSVCS sample is magnitude limited for $M_B < -18.94$. Nine of the 26 galaxies in this magnitude range (35%) have a significant system of DSCs. This is partially driven by the high fraction of S0s in this magnitude range. However, of the 38 ACSVCS galaxies with S0 classifications in the VCC, these nine are the only ones with significant DSC systems (24% of S0s). Given that of the 63 galaxies that were removed from the ACSVCS sample a large number were S0s, it is difficult to determine the true DSC frequency.

4. *DSCs are spatially aligned with the galaxy light.* In cases where a galaxy is highly inclined or the galaxy light is anisotropic within the ACS field of view, the DSCs visibly align themselves with the galaxy. It is likely that the DSCs are a population of star clusters associated with the disks of galaxies, rather than with bulges or halos. Although Larsen & Brodie (2000) use deep WFPC2 data to claim that there is a deficit of "faint fuzzies" at the center of NGC 1023, we are not able to make a similar statement about the DSC populations due to rising incompleteness in the high surface brightness central regions of some of our galaxies, and so we cannot comment on the frequency of "ring" structures such as those simulated by Burkert, Brodie, & Larsen (2005).

5. *The fraction of stellar luminosity contained in diffuse star clusters for our DSC-excess sample is typically* $1–7 \times 10^{-4}$. VCC 9 and VCC 1199 are the exceptions. It is possible that the lower luminosity galaxies in the sample also have DSCs, but if they form at similar efficiencies, then it would be difficult to notice them among the background contamination. However, the central regions of the giant ellipticals are definitely deficient in DSCs.

6. *Most DSC systems are associated with galactic disks, but many lenticulars do not host substantial DSC populations.* Both the spatial distributions of the diffuse clusters and the morphological classification of their host galaxies suggest that the formation and sustainability of DSCs is linked to the existence of a stellar disk. Nine of the 12 galaxies with significant diffuse star cluster populations are morphologically classified as S0 (11 out of 14 if one counts VCC 1154 and 2092). The existence of similar clusters in the spiral galaxies studied by Chandar et al. (2004) provides more evidence that disks are preferred environments for the formation and survival of diffuse star clusters. However, not all disks harbor DSCs, and in fact the majority of the lenticulars in our sample do *not* have substantial diffuse star cluster systems. One clue is that DSCs seem to exist preferentially in galaxies with visible dust—five of the nine S0s with substantial DSC populations also have visible dust at their centers. Understanding the variations in DSC numbers between galaxies that are otherwise very similar will be important for determining the origin of diffuse star clusters.

7. *There may be more than one mode of diffuse cluster formation.* Two notable exceptions in our sample are not lenticular galaxies. VCC 9 is an isolated low surface brightness dwarf elliptical galaxy that has a central concentrated population of DSCs. The existence of DSCs in the dwarf spheroidals of the Sharina et al. (2005) sample also suggest that DSCs can form outside of the disk environment (or that the dSphs previously had disks).

8. *Environment does not appear to predict of the existence of a diffuse star cluster population.* We find that there is little trend between clustercentric radius or local galaxy density with the number of DSC candidates. Although some of the galaxies with DSCs have nearby neighbors (VCC 798 and 1030), others are isolated. The old ages of the DSCs also argue against an important role for very *recent* interactions. Nevertheless, the fact that a VCC 798 and 1030 have close neighbors and that the existence of dust may be important are both signs that interactions may be one avenue for the formation of diffuse star clusters.

9. *The lack of many known DSC analogs in the Milky Way does not mean they do not exist.* Given the difficulty of searching the Galactic plane for low surface brightness star clusters, we estimate that the Galaxy could have a DSC-like star cluster population and only a few would have been within the range of previous surveys.

10. *The old open clusters are the closest Galactic counterpart to the diffuse star clusters.* These relatively metal-rich disk clusters are similar to the DSCs we observe, but are generally less luminous and probably younger.

Future observations will further elucidate the origins of these diffuse star cluster populations. The ACS Fornax Survey will image 43 early-type galaxies to similar depths as the ACSVCS, but in a different environment (Jordán et al. 2006). We are also obtaining deep optical

and near-infrared photometry of hundreds of star clusters in VCC 798 for the purpose of constraining their ages, metallicities, and structural parameters.

We thank Sidney van den Bergh for making his catalog of open clusters available to us before publication. We also thank Arunav Kundu for sending us his photometry of M87 globular clusters. Support for program GO-9401 was provided through a grant from the Space Telescope Science Institute, which is operated by the Association for Research in Astronomy, Inc., under NASA contract NAS5-26555. Partial support for this work was provided by NASA LTSA grant NAG5-11714 to PC. M. J. W. acknowledges support through NSF grant AST 02-05960. This research has made use of the NASA/IPAC Extragalactic Database (NED) which is operated by the Jet Propulsion Laboratory, California Institute of Technology, under contract with the National Aeronautics and Space Administration. This research has made use of the Vizier catalog service (Ochsenbein et al. 2000), which is hosted by the Centre de Données astronomiques de Strasbourg.

Facilities: HST(ACS)

REFERENCES

Bertin, E., & Arnouts, S. 1996, A&AS, 117, 393
Bica, E., Dutra, C. M., & Barbuy, B. 2003, A&A, 397, 177
Binggeli, B., Sandage, A., & Tammann, G. A. 1985, AJ, 90, 1681 (BST85)
Brodie, J. P., & Larsen, S. S. 2002, AJ, 124, 1410
Bruzual, G., & Charlot, S. 2003, MNRAS, 344, 1000
Burkert, A., Brodie, J., & Larsen, S. 2005, ApJ, 628, 231
Chabrier, G. 2003, PASP, 115, 763
Chandar, R., Bianchi, L., & Ford, H. C. 1999, ApJ, 517, 668
Chandar, R., Bianchi, L., & Ford, H. C. 2001, A&A, 366, 498
Chandar, R., Bianchi, L., Ford, H. C., & Sarajedini, A. 2002, ApJ, 564, 712
Chandar, R., Whitmore, B., & Lee, M. G. 2004, ApJ, 611, 220
Côté, P., et al. 2004, ApJS, 153, 223 (Paper I)
de Vaucouleurs, G., de Vaucouleurs, A., Corwin, H. G., Buta, R. J., Paturel, G., & Fouque, P. 1991, Volume 1-3, XII, 2069 pp. 7 figs.. Springer-Verlag Berlin Heidelberg New York,
Dias, W. S., Alessi, B. S., Moitinho, A., & Lépine, J. R. D. 2002, A&A, 389, 871
Fall, S. M., & Rees, M. J. 1977, MNRAS, 181, 37P
Fall, S. M., & Zhang, Q. 2001, ApJ, 561, 751
Ferrarese, L., et al. 2005, submitted (Paper VI)
Ford, H. C., et al. 1998, Proc. SPIE, 3356, 234
Friel, E. D. 1995, ARA&A, 33, 381
Freedman, W. L., et al. 2001, ApJ, 553, 47
Gebhardt, K., & Kissler-Patig, M. 1999, AJ, 118, 1526
Gomez, M., Geisler, D., Harris, W. E., Richtler, T., Harris, G. L. H., & Woodley, K. 2005, ArXiv Astrophysics e-prints, arXiv:astro-ph/0510544
Harris, W. E. 1996, AJ, 112, 1487
Haşegan, M., et al. 2005, ApJ, 627, 203 (Paper VII)
Haşegan, M., et al. 2006, in prep
Hilker, M., Infante, L., Vieira, G., Kissler-Patig, M., & Richtler, T. 1999, A&AS, 134, 75
Huxor, A. P., Tanvir, N. R., Irwin, M. J., Ibata, R., Collett, J. L., Ferguson, A. M. N., Bridges, T., & Lewis, G. F. 2005, MNRAS, 360, 1007
Janes, K. A., & Phelps, R. L. 1994, AJ, 108, 1773
Jordán, A., et al. 2004a, ApJS, 154, 509 (Paper II)
Jordán, A., et al. 2004b, ApJ, 613, 279 (Paper III)
Jordán, A., et al. 2005a, ApJ, in press, arXiv:astro-ph/0508219, (Paper X)
Jordán, A., et al. 2005b, ApJ, in prep
Koekemoer, A. M., Fruchter, A. S., Hook, R. N., & Hack, W. 2002, The 2002 HST Calibration Workshop : Hubble after the Installation of the ACS and the NICMOS Cooling System, Proceedings of a Workshop held at the Space Telescope Science Institute, Baltimore, Maryland, October 17 and 18, 2002. Edited by Santiago Arribas, Anton Koekemoer, and Brad Whitmore. Baltimore, MD: Space Telescope Science Institute, 2002., p.339, 339
Kundu, A., Whitmore, B. C., Sparks, W. B., Macchetto, F. D., Zepf, S. E., & Ashman, K. M. 1999, ApJ, 513, 733
Larsen, S. S., & Richtler, T. 2000, A&A, 354, 836
Larsen, S. S., & Brodie, J. P. 2000, AJ, 120, 2938
Larsen, S. S., Brodie, J. P., Huchra, J. P., Forbes, D. A., & Grillmair, C. J. 2001, AJ, 121, 2974
Mei, S., et al. 2005, ApJ, 625, 121 (Paper V)
Ochsenbein, F., Bauer, P., & Marcout, J. 2000, A&AS, 143, 23
Peng, E. W., et al. 2005, ApJ, in press, arXiv:astro-ph/0509654, (Paper IX)
Schlegel, D. J., Finkbeiner, D. P., & Davis, M. 1998, ApJ, 500, 525
Sharina, M. E., Puzia, T. H., & Makarov, D. I. 2005, ArXiv Astrophysics e-prints, arXiv:astro-ph/0505624, å, accepted
Sirianni, M., Jee, M.J., Bentez, N., Blakeslee, J.P., Martel, A.R., Meurer, G., Clampin, M., De Marchi, G., Ford, H.C., Gilliland, R., Hartig, G.F., Illingworth, G.D., Mack, J., & McCann, W.J. 2005, PASP, accepted
Tonry, J. L., Dressler, A., Blakeslee, J. P., Ajhar, E. A., Fletcher, A. B., Luppino, G. A., Metzger, M. R., & Moore, C. B. 2001, ApJ, 546, 681
van den Bergh, S., & Mackey, A. D. 2004, MNRAS, 354, 713
van den Bergh, S. 2005a, ArXiv Astrophysics e-prints, arXiv:astro-ph/0509811, AJ, in press
van den Bergh, S. 2005b, submitted